Society For Biomaterials

Design and characterization of a conductive nanostructured polypyrrole-polycaprolactone coated magnesium/PLGA composite for tissue engineering scaffolds

Haixia Liu,[1,2]* Ran Wang,[1]* Henry K. Chu,[1] Dong Sun[1]

[1]Department of Mechanical and Biomedical Engineering, City University of Hong Kong, Kowloon Tong, Hong Kong
[2]School of Instrument Science and Optoelectronic Engineering, Beihang University, Beijing 100191, China

Received 28 November 2014; revised 5 February 2015; accepted 5 February 2015
Published online 11 March 2015 in Wiley Online Library (wileyonlinelibrary.com). DOI: 10.1002/jbm.a.35428

Abstract: A novel biodegradable and conductive composite consisting of magnesium (Mg), polypyrrole-*block*-ploycaprolactone (PPy-PCL), and poly(lactic-*co*-glycolic acid) (PLGA) is synthesized in a core-shell-skeleton manner for tissue engineering applications. Mg particles in the composite are first coated with a conductive nanostructured PPy-PCL layer for corrosion resistance via the UV-induced photopolymerization method. PLGA matrix is then added to tailor the biodegradability of the resultant composite. Composites with different composition ratios are examined through experiments, and their material properties are characterized. The *in vitro* experiments on culture of 293FT-GFP cells show that the composites are suitable for cell growth and culture. Biodegradability of the composite is also evaluated. By adding PLGA matrix to the composite, the degrading time of the composite can last for more than eight weeks, hence providing a longer period for tissue formation as compared to Mg composites or alloys. The findings of this research will offer a new opportunity to utilize a conductive, nanostructured-coated Mg/PLGA composite as the scaffold material for implants and tissue regeneration. © 2015 Wiley Periodicals, Inc. J Biomed Mater Res Part A: 103A: 2966–2973, 2015.

Key Words: conductive scaffold, tissue engineering, PPy-PCL, magnesium, nanostructured coating

How to cite this article: Liu H, Wang R, Chu HK, Sun D. 2015. Design and characterization of a conductive nanostructured polypyrrole-polycaprolactone coated magnesium/PLGA composite for tissue engineering scaffolds. J Biomed Mater Res Part A 2015:103A:2966–2973.

INTRODUCTION

Artificial tissue regeneration has emerged as a promising approach to repairing damaged or diseased tissues in human body. To produce three-dimensional (3D) tissue construction, the fabrication process usually requires a polymeric scaffold as a temporary platform for cells to adhere and proliferate. Hence, the polymeric scaffold material needs to be biocompatible and biodegradable such that cell growth, proliferation, and differentiation can be allowed.[1,2] In addition, the scaffold material should be stiff enough for practical handling.[3] Recent studies have shown that human tissues possess different dielectric properties[4–6] and the presence of electrical signal can play an integral role in cell behavior and tissue formation.[7–9] For instance, electrical stimulation has been found to be effective to enhance cell adhesion,[10] cell differentiation,[11,12] wound healing,[13] protein secretion,[14] and DNA synthesis of electrically responsive cells.[15–17] Our recent research also shows that electric field can be utilized as the active cell seeding mechanism to manipulate a large amount of cells toward the scaffold body.[18] Therefore, synthesizing a conductive biomaterial that can be used for the above electrical micro-environment would have great potential to accelerate the tissue culture and development processes.

As one of the most abundant minerals in the body, magnesium (Mg) is essential to many cellular biochemical reactions such as energy metabolism, protein synthesis, and maintenance of the electrical potential of cell membranes.[19] Some studies have shown that the use of magnesium supplementation may help reduce blood pressure[20,21] and facilitate bone regeneration.[22] With excellent mechanical properties and biocompatibility in human body, magnesium has been increasingly used as the biomaterial for medical implant applications.[23] To date, a number of magnesium-based scaffolds have been reported by different research groups.[24–27] Nevertheless, many of them mainly used

*These authors contributed equally to this work
Correspondence to: D. Sun; e-mail: medsun@cityu.edu.hk
Contract grant sponsor: Research Grants Council of the Hong Kong Special Administrative Region, China; contract grant number: CityU09/CRF/13G
Contract grant sponsor: Beijing Natural Science Foundation; contract grant number: 7152089
Contract grant sponsor: China Postdoctoral Science Foundation; contract grant number: 2013M540036

magnesium fibers or magnesium sheet as the material, which are hard to be handled by conventional microfabrication techniques such as solid freeform fabrication (SFF) or 3D printing to construct complicated 3D structure that is necessary for cell culture. Some investigations were performed recently for producing a topologically ordered Mg-biopolymer hybrid 3D composite structure,[28,29] but the formed 3D structure was found to have a higher corrosion rate due to polymer breakdown.

Magnesium is a known reactive metal that is vulnerable to oxidation and other chemical reactions. Magnesium can react with water to produce magnesium ions that lead to a pH increase in the cell culture medium. Its fast degradation rate also makes it difficult to meet the specific requirement for clinical applications.[30–32] The key challenge for Mg-based medical implants lies in the control of material stability and degradation in a physiological environment. Surface modification via coating can be a viable solution, and examples of the coating materials include poly(lactic-*co*-glycolic acid) (PLGA),[33] poly caprolactone (PCL),[34]and different conductive polymers (CPs).[35–37] Polypyrrole (PPy) is a well-studied CP for tissue engineering because it possesses good electrical conductivity, biocompatibility, and high electrical stability.[38,39] Mg alloy protection through coating of PPy powders was examined.[24] A recent study demonstrated that a block copolymer composed of PPy and PCL exhibited better conductivity, biodegradability, and ability to support PC12 cell proliferation.[40] PPy itself is generally non-degradable with limited manufacturability of complex 3D structures. Composite materials have the advantages of tailoring the material properties by adjusting the ratio among the materials. Some investigations have been performed recently for producing conductive composites such as Mg-PPy,[24] PLGA-Mg,[25,33] and PLGA-PPy.[38,39]

This article reports a new approach to synthesizing a novel composite that consists of Mg particles, PPy-PCL, and PLGA in a core-shell-skeleton manner. Mg particles were chosen as the conductive cores. Conductive polymer PPy-PCL was polymerized to form a nanostructured shell that encapsulates Mg particles from corrosion and oxidization. PLGA was used as the skeleton of the copolymer composite to provide controllability on the degradation rate. The material properties of the composite were characterized. Cell culture experiments were conducted on such a new composite, and the results demonstrated that this new composite exhibited excellent biomaterial properties, electrical conductivity, and good mechanical property for tissue engineering scaffolds. Findings of this study will lead generation of a new biomaterial that can be both conductive and biodegradable for a broad range of tissue engineering applications.

MATERIALS AND METHODS

Materials

The following materials, purchased from Sigma-Aldrich, were used in this study: PPy-PCL (polypyrrole-*block*-poly (caprolactone), biodegradable block copolymers containing *p*-toluenesulfonate as dopant, 0.3–0.7 wt % in nitromethane), Mg(Granular, 20–230 mesh, 98% Mg, reagent grade), poly(lactic-glycolic acid) (PLGA, ratio M/M% 50:50, MW 30,000–60,000Da), dichloromethane(Anhydrous), acetone ($\geq$99.9%), phosphate buffered saline (PBS) tablets, and 0.5*M* hydrochloric acid. All other chemicals were analytical grade and were used as received.

TABLE I. Concentration of PPy-PCL, PLGA, and Mg in the Composites

Composite	Composition	PPy solution (mL)	Mg (mg)	PLGA (mg)
A1	1Py10 Mg	1	10	
A2	1Py20 Mg	1	20	
A3	2Py10 Mg	2	10	
B1	1Py10 Mg4PG	1	10	4
B2	1Py20 Mg4PG	1	20	4
B3	2Py10 Mg8PG	2	10	8

Preparation of nanostructured PPy-PCL coated Mg particles

The UV-induced polymerization method was used for coating PPy-PCL on the Mg particles. Prior to each experiment, Mg particles were immersed in 0.5 mol/L hydrochloric acid for 30 s to remove the oxide layer on the surface. The particles were rinsed and kept in acetone before use. The photopolymerization process was carried out by dispersing the Mg particles into the PPy-PCL solution under a fume hood. Based on the work,[41] the mixture was exposed to a 254 nm UV lamp (500 W) and simultaneously stirred with a magnetic stirrer at 500 R.P.M. until dried. UV irradiation was used to enhance the polymerization of polypyrrole when depositing onto the Mg particles. The dried Mg particles were further exposed to the UV lamp for 24 h at room temperature (RT). The photopolymerized Mg particles were washed twice with ethanol and dried under vacuum. In this work, the composition ratio between the Mg particles and the PPy-PCL solution was examined in order to characterize their influence on the resultant Mg particles. Table I summarizes the parameters used in the experiment.

Preparation of nanostructured PPy-PCL coated mg and PLGA composite

To fabricate the PPy-PCL coated Mg-PLGA composite scaffolds, PLGA powders were first dissolved in dichloromethane (CH_2Cl_2) to prepare a 10% (weight/volume) PLGA stock solution. Then, PPy-PCL coated Mg particles were added into the PLGA solution. The mixture was placed under vacuum to allow the PLGA solution to infiltrate into the porous PPy-PCL coated Mg aggregates, resulting in the formation of the PPy-PCL coated Mg and PLGA composite. The composite mixture was then cast into a Teflon petri dish and sonicated for 10 min (W-385, Farmingdale). After sonication, the composite was dried in a fume hood for overnight. The composite was further dried in an oven at 45 °C for 6 h and stored at room temperature for at least 2

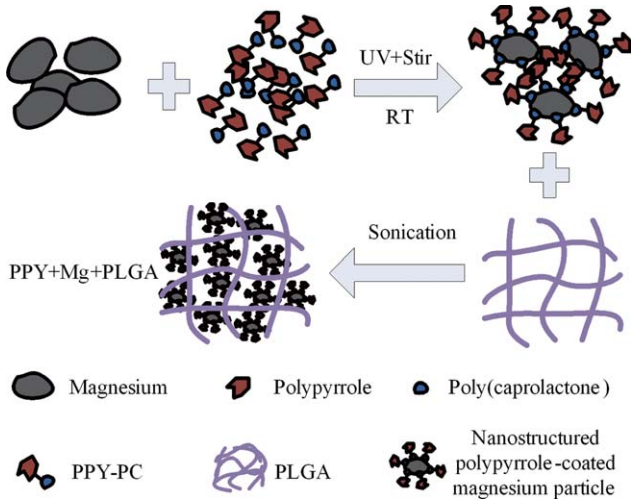

FIGURE 1. Schematic illustration for preparing the nanostructured PPy-PCL coated Mg particle and PLGA composite in a core-shell-skeleton manner. [Color figure can be viewed in the online issue, which is available at wileyonlinelibrary.com.]

days to evaporate all organic solvents. Figure 1 illustrates a schematic of the fabrication procedure for the nanostructured PPy-PCL coated Mg and PLGA composite. Composites with different composition ratios were prepared to evaluate their influence on the material properties and *in vitro* cell culture. Table I summarizes the amount of each material used during the photopolymerization and the composite synthesis processes. Prior to the experiments, each sample was treated with a plasma cleaner (PDC-002, 13.56 MHz RF Plasma) to enhance the surface hydrophilicity for cell attachment and cell growth.[42] The pressure of the vacuum chamber was set to around 800 mTorr and the samples were exposed to the plasma from 45 W RF coil for 15 min.

The size and morphology of each composite were characterized using scanning electron microscopy (JSM-5600, JEOL Ltd). The accelerating voltage was set to 20 kV. To evaluate the repeatability of the results, three samples were tested per each composite group ($n = 3$), unless otherwise specified.

Mechanical testing

The compressive yield strength of each composite was measured using a micro hardness tester (Fischerscope HM 2000 XYp). The composites prepared in section "Preparation of nanostructured PPy-PCL coated Mg and PLGA composite" were first cut into pieces of 25 mm by 25 mm, with a thickness of ~0.8 mm. Before the testing, each sample piece was placed under a hydraulic press at 5 MPa for 10 min to enhance the surface uniformity. A test load of 100 mN was applied to the sample and the indentation depth was recorded. Based on the information, the unloading curve of each sample was plotted and the modulus of elasticity, E, was then calculated by Power Law Method. The modulus was averaged from the three samples of each group.

Conductivity measurement

The resistivity of the each composite was measured using the method as described.[43] Two metal electrodes that were 10 mm apart were first attached to a polydimethylsiloxane (PDMS) substrate and the electrodes were connected to a Digital Multimeter (2100/120, Keithley Instruments). Hydrated samples that are 10 mm long with a cross-sectional area of 0.8 mm × 0.8 mm were tightly clamped between the two electrodes for the measurement. The resistance measurement (R) was carried out six times on each sample. The average conductivity, which is the inverse of the resistivity (p), was calculated using the Pouillet's law Eq. (1):

$$R = \frac{pL}{A} \tag{1}$$

where L is length and A is the cross-sectional area of the sample.

In vitro degradation measurement

In vitro degradation studies were performed by measuring the weight loss of the samples at different time during the incubation. All samples were sterilized with ethyl alcohol (>99%) for 2 min, and rinsed twice with PBS before transferring to 12-well tissue culture plates for subsequent incubation. Dulbecco's Modified Eagle's Medium (DMEM) with 1% penicillin and streptomycin (Sigma-Aldrich) were added to each well to completely cover the sample surface and the plates were incubated at 37 °C and 5% CO_2 for up to 8 weeks. At each predetermined interval, samples from each group were collected from the plate. The samples were washed with deionized water and then freeze-dried to measure the residual weight.

Cell viability and proliferation

A series of cell culture experiments were performed to examine the effects of different composition ratios on cell viability and proliferation. Sterilized samples were first transferred to a 24-well culture plate that was pre-coated with bovine serum albumin (BFA) to minimize cell attachment. Human kidney cells, 293FT, were stably transfected with a green fluorescent protein (GFP) plasmid and then pipetted onto the sterilized samples at a concentration of 5×10^4 cells. Following cell attachment at 37°C for 30 min, DMEM culture medium was added to the plate and the medium was exchanged every two to three days. To characterize the cells after culture, hydrated samples seeded with cells were first fixed with 4% paraformaldehyde (Sigma-Aldrich) for 20 min. The samples were then washed with PBS and dehydrated through an automated critical point dryer (CPD300, Leica Microsystems Ltd). The samples were sputter-coated with a 10 nm gold layer using a Quorum Coater (Q150TS, Quorum Technologies Inc.).

RESULTS

Microstructure, elemental composition, and size of PPy-PCL coatings

Material samples as prepared in the previous Section were characterized using scanning electron microscopy (SEM). Images obtained confirm that PPy-PCL was successfully coated onto the Mg particles via the photopolymerization

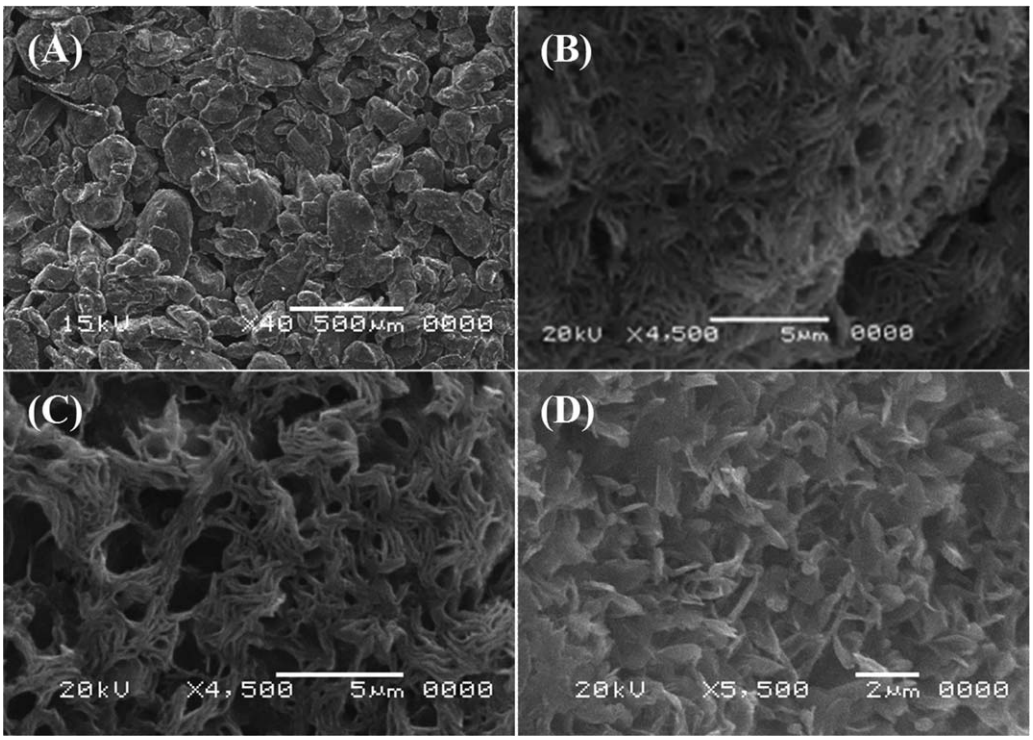

FIGURE 2. SEM images of nanostructured PPy-PCL coated Mg particles. A: 1Py10 Mg at low magnification (scale bar: 500 μm). B: 1Py10 Mg at high magnification (scale bar: 5 μm). C: 1Py20 Mg at high magnification (scale bar: 5 μm). D: 2Py10 Mg prepared at high magnification (scale bar: 2 μm).

method. Figure 2(A) shows the surface morphology of the material from PPy-PCL coated Mg particles (sample A1). Under a ×4500 magnification, the PPy-PCL coating was found to have a relatively porous, nanoscale architecture [Fig. 2(B)].

Material properties

Table II summarizes the elastic modulus of each composite obtained from the mechanical compression testing. The densities were evaluated by measuring the dimensions and the weight of each sample. Among the three materials in the composite, Mg has the highest elastic modulus and the resultant modulus of the composite has a strong dependency on its ratio in the composite. For a typical bone tissue, the elastic modulus is around 0.12–0.5 GPa but the elastic modulus of PPy-PCL coated Mg is 18 ± 0.1 GPa. After adding PLGA into the composite, the average elastic modulus was reduced to 0.26 ± 0.01 GPa (composite B1), which was more favorable for tissue engineering application.

The conductivity of the three Mg-PPy-PLGA composites were also measured and shown in Table II. Composite B1 has a conductivity of 45 S/m. The conductivity of composite B2 increased to 54 S/m due to a higher Mg content. Composite B3, which has the highest PLGA content, has a conductivity of only 41 S/m.

Degradation measurement

The degradation rate of the composite in DMEM medium was further examined. Figure 3 shows the change of the surface morphology of the composite B3 for 4 weeks. Before the experiment, the composite surface was mainly composed of PLGA matrix. After one week, cracks can hardly be seen on the PLGA surface, but more pores can be found. The PLGA matrix degraded faster after two weeks, and PPy-PCL coated Mg particles that were originally encapsulated by PLGA became exposed to the medium. After four weeks, PLGA started to lose its integrity and PLGA fragment were observed on the surface. Coated-Mg particles were also found to be corroded by the medium. The remaining weights of this composite B3, as well as the other two composites B1 and B2, were all measured and plotted in Figure 4. The results showed that the ratio of the PLGA matrix in the composite has a significant influence on the degradation behavior. After the first week, the percentages of average weight loss

TABLE II. Mechanical and Conductive Properties of Composites in Comparison With Spongy Bone

Scaffold	Modulus (E) (GPa)	Density(ρ) (g/cm^3)	Specific modulus (E/ρ)	Conductivity (S/m)
Spongy bone[5,42]	0.12–0.5	0.14–1.2	~0.5	0.01–0.06
1Py10 Mg4PG (B1)	0.26 ± 0.01	1.35 ± 0.03	0.19	45 ± 2
1Py20 Mg4PG (B2)	0.38 ± 0.01	1.45 ± 0.04	0.26	54 ± 2
2Py10 Mg8PG (B3)	0.31 ± 0.01	1.38 ± 0.05	0.23	41 ± 2

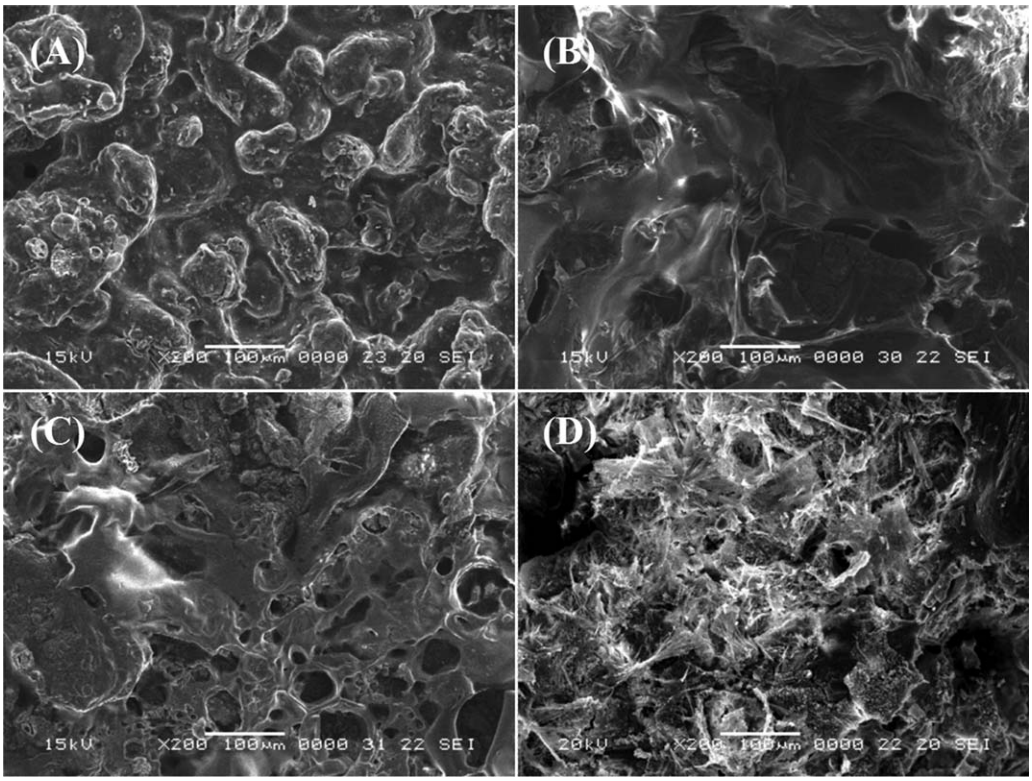

FIGURE 3. Surface morphology of the 2Py10 Mg8PG composite (B3) after immersing in DMEM solution. A: Zero. B: One week. C: Two weeks. D: Four weeks. Scale bar are 100 μm.

for B1, B2, and B3 were 2%, 3%, and 1%, respectively. After two weeks, the degradation increased and the composite with low PLGA content and thinner coating (B2) has the highest degradation rate. The composite B3 still had at least 50% of the weight after four weeks. Another 0.7 mm thickness composite 1Py10 Mg (A1), without PLGA, was also fabricated and kept in DMEM as a control. This composite completely degraded in 4 weeks (9.6 mm/year). While the composites of PPy-PCL coated Mg with PLGA (B1, B2 and B3) were not completely degraded even after 8 weeks.

In vitro cell culture and proliferation

The composites with PLGA covalently conjugated onto the nanostructured PPy-PCL coated Mg particles were examined *in vitro* for cell culture. Each composite seeded with 293FT-GFP cells was cultured for 5 days and the composites were observed under fluorescent microscopy (FM) and SEM every two days. The results (Fig. 5) show that 293FT-GFP cells were successfully adhered and proliferated throughout the composites. The coverage of the fluorescent green 293FT-GFP cells were quantified using image analysis software, and the data were plotted in Figure 6. Among the three composites (B1, B2, B3) with different composition ratios, B3 appears to be the most suitable substrate for cell culture and the cells proliferated at a rate of 4.6 times in 120 h. The composite B1 has a proliferation rate of 4.3 times while B2 has a rate of four times. This result can be explained by the change of pH value of the culture medium. A pH meter (SB70P, VWR International) was used to measure the pH values of the post-culture media, and the results are shown in Figure 7. The pH values of B1 and B3 are close to that of the culture medium (control) in the incubator. In contrast, the pH value of B2 increases from 7.4 to 7.8, indicating a more alkaline solution due to the corrosion of the Mg particles.

DISCUSSIONS

Composition ratios affect the architecture and properties of material

The above results indicate that the composition ratio would have an influence on the architecture of the coating. As the

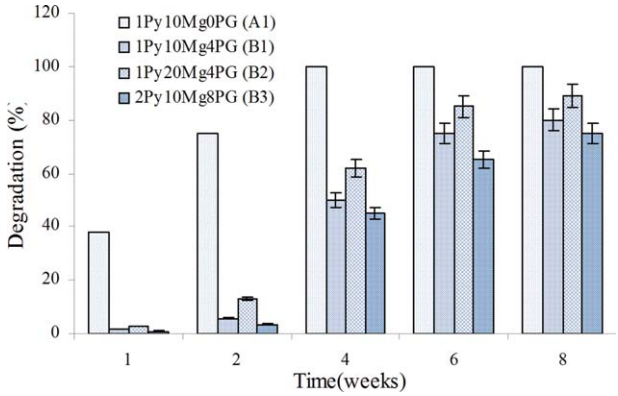

FIGURE 4. *In vitro* degradation of the control and the three composites: 1Py10 Mg4PG, 1Py20 Mg4PG, and 2Py10 Mg8PG (mean ± standard deviation, n = 3) over eight weeks. [Color figure can be viewed in the online issue, which is available at wileyonlinelibrary.com.]

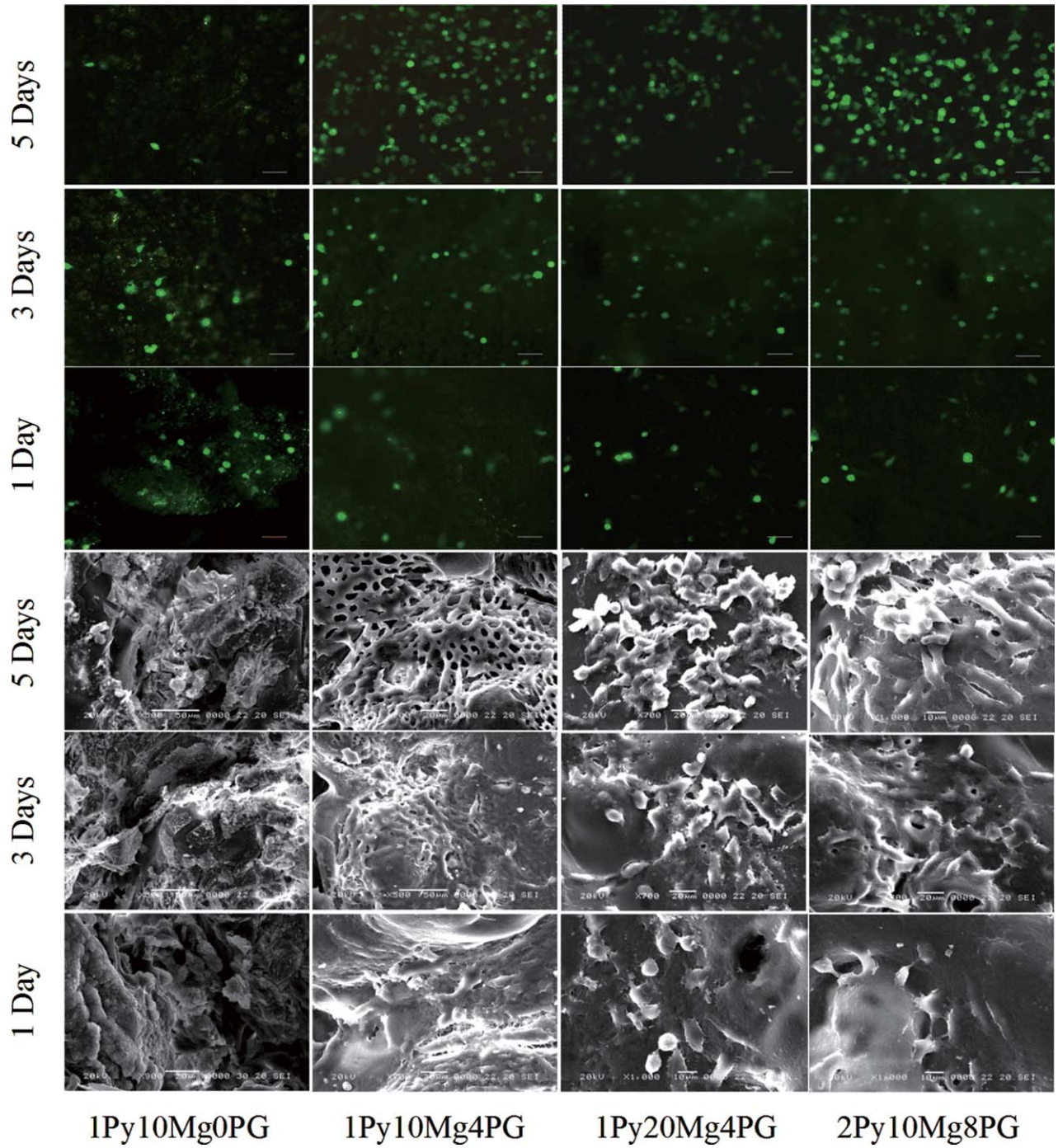

FIGURE 5. FM and SEM images of 293FT-GFP cells on different composite surfaces over the culture period (scale bar: 100 μm in FM, 10–50 μm in SEM). [Color figure can be viewed in the online issue, which is available at wileyonlinelibrary.com.]

content of the Mg particle increases, the coating becomes more porous and the average pore size changes from ~2 μm [sample A1, Fig. 2(B)] to 5 μm [sample A2, Fig. 2(C)]. In contrast, increasing the content of the PPy-PCL solution leads to a denser surface coating [sample A3, Fig. 2(D)], and hence, pores are barely visible and the average size reduces to less than 0.5 μm.

Increasing the Mg ratio can also enhance the elastic modulus of the resultant composite, which was evidenced by the increased modulus for composite B2, that is 0.38 ± 0.01 GPa. The mechanical properties of all the three composites, 1Py10 Mg4PG (B1), 1Py20 Mg4PG (B2), and 2Py10 Mg8PG (B3), are comparable to a bone in human, which can provide sufficient mechanical strength to resist contractile forces after scaffold implantation.

The conductivity of the three Mg-PPy-PLGA composites indicates that the conductivity is dependent on the amount of the conductive PPy-PCL coated Mg filler in the composite.

In addition, all these composites are found to be more conductive than ventricular muscle, blood, and skeletal muscle in human (0.03 − 0.6 S/m),[44] demonstrating the feasibility of applying electrical signals or stimulations on these new biomaterials to accelerate the tissue regeneration.

Controlling mg degradation through PPy-PCL coatings better cell proliferation

The composite 1Py10 Mg (A1, without PLGA, 0.7 mm thickness sample) is completely degraded in four weeks (9.6 mm/year). While the composites of PPy-PCL coated Mg with PLGA (B1, B2, and B3) were not completely degraded even after 8 weeks. This result is comparable with the degradation rate of pure magnesium (10.5–39 mm/year), depending on the medium used and the material porosity.[27,35] Therefore, PPy-PCL coated magnesium has better corrosion resistance than pure magnesium, and adding PLGA can enhance the stability and biodegradation resistance of the composite.

Mg particles in the composite react with the aqueous environment to form magnesium hydroxide. This hydrogenation causes the pH to increase and hence affects the cell culture.[45] This result agrees to the degradation study that the composite B2 has the fastest degradation rate among the three composites.

CONCLUSIONS

A biodegradable and conductive composite consisting of Mg, PPy-PCL, and PLGA was designed and fabricated. Three composites with different composition ratios were characterized for potential tissue engineering applications. Mechanical and biodegradability tests were conducted and the correlations among the three materials on the resultant composite were investigated. The results indicated that the use of Mg particles coated with conductive PPy-PCL can provide electrical conductivity to the resultant composite. Composites with high magnesium contents can improve the overall elastic modulus. Composites with high PLGA contents can extend the degradation time. *In vitro* experiments of culturing 293FT-GFP cells were conducted on the composites, and the cells were found to be proliferated and uniformly spread throughout the composite surface. The results indicate that the newly designed biodegradable and conductive Mg-PPy-PLGA composites can be used for fabricating tissue engineering scaffolds, as well as other tissue engineering applications such as electrical stimuli and DEP cell pattern to enhance tissue regeneration.

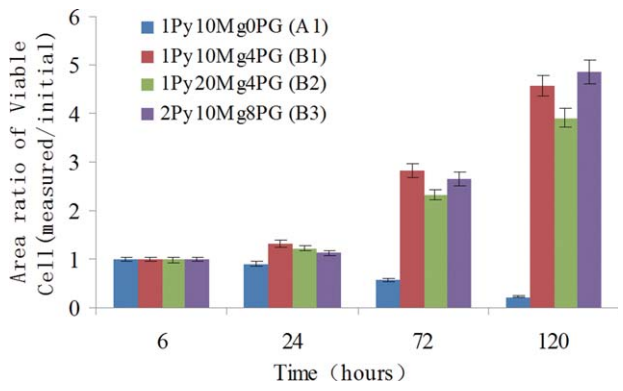

FIGURE 6. The results of cell proliferation. The area ratio covered by viable 293FT-GFP cells on the 1Py10 Mg0PG, 1Py10 Mg4PG, 1Py20 Mg4PG, and 2Py10 Mg8PG composites. [Color figure can be viewed in the online issue, which is available at wileyonlinelibrary.com.]

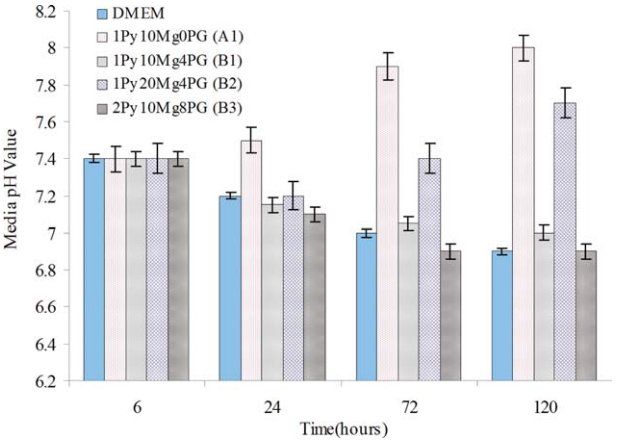

FIGURE 7. The pH values of the post-culture media. Average pH values of the post-culture media from the 1Py10 Mg0PG, 1Py10 Mg4PG, 1Py20 Mg4PG, and 2Py10 Mg8PG composites at different intervals. [Color figure can be viewed in the online issue, which is available at wileyonlinelibrary.com.]

REFERENCES

1. Muskovich M, Bettinger CJ. Biomaterials-based electronics: Polymers and interfaces for biology and medicine. Adv Healthcare Mater 2012;1:248–266.
2. Ma PX. Biomimetic materials for tissue engineering. Adv Drug Deliv Rev 2008;60:184–198.
3. Ceyssens F, van Kuyck K, Vande Velde G, Welkenhuysen M, Stappers L, Nuttin B, Puers R. Resorbable scaffold based chronic neural electrode arrays. Biomed Microdevices 2013;15:481–493.
4. Gabriel C, Gabriel S, Corthout E. The dielectric properties of biological tissues. I. Literature survey. Phys Med Biol 1996; 41:2231–2249.
5. Gabriel S, Lau RW, Gabriel C. The dielectric properties of biological tissues. II. Measurements in the frequency range 10 hz to 20 GHz. Phys Med Biol 1996;41:2251–2269.
6. Yao C, Li Q, Guo J, Yan F, Hsing IM. Rigid and flexible organic electrochemical transistor arrays for monitoring action potentials from electrogenic Cells. Adv Healthcare Mater 2014. DOI:10.1002/adhm.201400406.
7. Yow SZ, Lim TH, Yim EKF, Lim CT, Leong KW. A 3D electroactive polypyrrole-collagen fibrous scaffold for tissue engineering. Polymers 2011;3:527–544.
8. Ateh DD, Vadgama P, Navsaria HA. Culture of human keratinocytes on polypyrrole-based conducting polymers. Tissue Eng 2006;12:645–655.
9. Ito A, Yamamoto Y, Sato M, Ikeda K, Yamamoto M, Fujita H, Nagamori E, Kawabe Y, Kamihira M. Induction of functional tissue-engineered skeletal muscle constructs by defined electrical stimulation. Sci Rep 2014;4. doi:10.1038/srep04781.
10. Sun S, Titushkin I, Cho M. Regulation of mesenchymal stem cell adhesion and orientation in 3D collagen scaffold by electrical stimulus. Bioelectrochemistry 2006;69:133–141.
11. Meng SY, Rouabhia M, Zhang Z. Electrical stimulation modulates osteoblast proliferation and bone protein production through heparin-bioactivated conductive scaffolds. Bioelectromagnetics 2013;34:189–199.
12. Vila M, Cicuendez M, Sanchez-Marcos J, Fal-Miyar V, Manzano M, Prieto C, Vallet-Regi M. Electrical stimuli to increase cell proliferation on carbon nanotubes/mesoporous silica composites for drug delivery. J Biomed Mater Res Part A 2013;101:213–221.

13. Yuan X, Arkonac DE, Chao PH, Vunjak-Novakovic G. Electrical stimulation enhances cell migration and integrative repair in the meniscus. Sci Rep 2014;4:3674.
14. Park H, Bhallal R, Saigal R, Radisic M, Watson N, Langer R, Vunjak-Novakovic G. Effects of electrical stimulation in C2C12 muscle constructs. J Tissue Eng Regen Med 2008;2:279–287.
15. Genovese JA, Spadaccio C, Langer J, Habe J, Jackson J, Patel AN. Electrostimulation induces cardiomyocyte predifferentiation of fibroblasts. Biochem Biophys Res Commun 2008;370:450–455.
16. Au HT, Cheng I, Chowdhury MF, Radisic M. Interactive effects of surface topography and pulsatile electrical field stimulation on orientation and elongation of fibroblasts and cardiomyocytes. Biomaterials 2007;28:4277–93.
17. Radisic M, Park H, Shing H, Consi T, Schoen FJ, Langer R, Freed LE, Vunjak-Novakovic G. Functional assembly of engineered myocardium by electrical stimulation of cardiac myocytes cultured on scaffolds. Proc Natl Acad Sci USA 2004;101:18129–18134.
18. Chu HK, Huan Z, Mills JK, Yang J, Sun D. Dielectrophoresis-based automatic 3D cell manipulation and patterning through a microelectrode integrated multi-layer scaffold. 14–18 Sept. 2014, Chicago, IL, USA: Intelligent Robots and Systems (IROS 2014), 2014 IEEE/RSJ International Conference on p 2003–2008. DOI:10.1109/IROS.2014.6942829.
19. Romani AM. Magnesium in health and disease. Met Ions Life Sci 2013;13:49–79.
20. Kass L, Weekes J, Carpenter L. Effect of magnesium supplementation on blood pressure: A meta-analysis. Eur J Clin Nutr 2012;66:411–418.
21. Jee SH, Miller ER, Guallar E, Singh VK, Appel LJ, Klag MJ. The effect of magnesium supplementation on blood pressure: A meta-analysis of randomized clinical trials. Am J Hypertens 2002;15:691–696.
22. Wu F, Su J, Wei J, Guo H, Liu C. Injectable bioactive calcium-magnesium phosphate cement for bone regeneration. Biomed Mater 2008;3:044105.
23. Brar HS, Platt MO, Sarntinoranont M, Martin PI, Manuel MV. Magnesium as a biodegradable and bioabsorbable material for medical implants. JOM 2009;61:31–34.
24. Singer F, Ruckle D, Killian MS, Turhan MC, Virtanen S. Electropolymerization and characterization of Poly-N-methylpyrrole coatings on AZ91D magnesium Alloy. Int J Electrochem Sci 2013;8:11924–11932.
25. Wu YH, Li N, Cheng Y, Zheng YF, Han Y. In vitro study on biodegradable AZ31 magnesium alloy fibers reinforced PLGA composite. J Mater Sci Technol 2013;29:545–550.
26. Li RW, Kirkland NT, Truong J, Wang J, Smith PN, Birbilis N, Nisbet DR. The influence of biodegradable magnesium alloys on the osteogenic differentiation of human mesenchymal stem cells. J Biomed Mater Res A 2014;102:4346–4357.
27. Zhang X, Li X-W, Li J-G, Sun X-D. Preparation and mechanical property of a novel 3D porous magnesium scaffold for bone tissue engineering. Mater Sci Eng C 2014;42:362–367.
28. Kirkland NT, Kolbeinsson I, Woodfield T, Dias GJ, Staiger MP. Synthesis and properties of topologically ordered porous magnesium. Mater Sci Eng B 2011;176:1666–1672.
29. Oosterbeek RN, Seal CK, Staiger MP, Hyland MM. Topologically ordered magnesium-biopolymer hybrid composite structures. J Biomed Mater Res A 2015;103:311–317.
30. Witte F. The history of biodegradable magnesium implants: A review. Acta Biomater 2010;6:1680–1692.
31. Xue DC, Yun YH, Tan ZQ, Dong ZY, Schulz MJ. In vivo and in vitro degradation behavior of magnesium alloys as biomaterials. J Mater Sci Technol 2012;28:261–267.
32. Johnson I, Liu H. A study on factors affecting the degradation of magnesium and a magnesium-yttrium alloy for biomedical applications. PLoS One 2013;8:e65603.
33. Johnson I, Akari K, Liu HN. Nanostructured hydroxyapatite/poly (lactic-*co*-glycolic acid) composite coating for controlling magnesium degradation in simulated body fluid. Nanotechnology 2013; 24. doi:10.1088/0957-4484/24/37/375103.
34. Wong HM, Yeung KWK, Lam KO, Tam V, Chu PK, Luk KDK, Cheung KMC. A biodegradable polymer-based coating to control the performance of magnesium alloy orthopaedic implants. Biomaterials 2010;31:2084–2096.
35. Sebaa MA, Dhillon S, Liu HN. Electrochemical deposition and evaluation of electrically conductive polymer coating on biodegradable magnesium implants for neural applications. J Mater Sci Mater Med 2013;24:307–316.
36. Luo XL, Cui XYT. Electrochemical deposition of conducting polymer coatings on magnesium surfaces in ionic liquid. Acta Biomater 2011;7:441–446.
37. Quigley AF, Razal JM, Kita M, Jalili R, Gelmi A, Penington A, Ovalle-Robles R, Baughman RH, Clark GM, Wallace GG and others. Electrical stimulation of myoblast proliferation and differentiation on aligned nanostructured conductive polymer platforms. Adv Healthcare Mater 2012;1:801–808.
38. Pelto J, Bjorninen M, Palli A, Talvitie E, Hyttinen J, Mannerstrom B, Suuronen Seppanen R, Kellomaki M, Miettinen S, Haimi S. Novel polypyrrole-coated polylactide scaffolds enhance adipose stem cell proliferation and early osteogenic differentiation. Tissue Eng Part A 2013;19:882–892.
39. Lee JY, Bashur CA, Goldstein AS, Schmidt CE. Polypyrrole-coated electrospun PLGA nanofibers for neural tissue applications. Biomaterials 2009;30:4325–4335.
40. Durgam H, Sapp S, Deister C, Khaing Z, Chang E, Luebben S, Schmidt CE. Novel degradable co-polymers of polypyrrole support cell proliferation and enhance neurite out-growth with electrical stimulation. J Biomater Sci Polym Ed 2010;21:1265–1282.
41. Yang XM, Lu Y. Preparation of polypyrrole-coated silver nanoparticles by one-step UV-induced polymerization. Mater Lett 2005;59: 2484–2487.
42. Shen H, Hu X, Yang F, Bei J, Wang S. Combining oxygen plasma treatment with anchorage of cationized gelatin for enhancing cell affinity of poly(lactide-co-glycolide). Biomaterials 2007;28:4219–4230.
43. Shahini A, Yazdimamaghani M, Walker KJ, Eastman MA, Hatami-Marbini H, Smith BJ, Ricci JL, Madihally SV, Vashaee D, Tayebi L. 3D conductive nanocomposite scaffold for bone tissue engineering. Int J Nanomed 2014;9:167–181.
44. Martins AM, Eng G, Caridade SG, Mano JF, Reis RL, Vunjak-Novakovic G. Electrically conductive chitosan/carbon scaffolds for cardiac tissue engineering. Biomacromolecules 2014;15:635–643.
45. Weng L, Webster TJ. Nanostructured magnesium has fewer detrimental effects on osteoblast function. Int J Nanomed 2013;8:1773–1781.